

# Electrical structure beneath the Hangai Dome, Mongolia: Magnetotelluric evidence for lithospheric melt and implications for uplift dynamics

M. J. Comeau<sup>1</sup>, J. S. Käuff<sup>2</sup>, M. Becken<sup>1</sup>, A. Kuvshinov<sup>2</sup>, S. Demberel<sup>3</sup>, U. Sukhbaatar<sup>3</sup>, E. Batmagnai<sup>3</sup>, S. Tserendug<sup>3</sup>, T. Nasan-Ochir<sup>3</sup>

<sup>1</sup> *Institut für Geophysik, Universität Münster, Münster, 48162, Germany*

<sup>2</sup> *Institute of Geophysics, Swiss Federal Institute of Technology (ETH), Zürich, 8092, Switzerland*

<sup>3</sup> *Institute of Astronomy and Geophysics of Mongolian Academy of Sciences, Ulaanbaatar, 13343, Mongolia*

**KEYWORDS:** magnetotellurics, Hangai dome, partial melt, uplift

## ABSTRACT

Important crust-mantle interactions are required to explain observations of intra-continental surface deformation and uplift far from tectonic plate boundaries, where deformation solely by means of plate tectonics is not possible. The Hangai Dome in central Mongolia is an unusual high-elevation, intra-continental plateau characterized by dispersed, low-volume volcanism. The processes responsible for developing the high topography remain unexplained, due in part to a lack of high-resolution geophysical data. Newly acquired broadband magnetotelluric data, the first in Mongolia, are used to generate an electrical resistivity model of the crust and upper mantle below the Hangai Dome. The lower crust contains anomalous discrete pockets of low-resistivity material that indicate the presence of fluids and possibly local accumulations of partial melt. These are spatially associated with surface expressions of late Cenozoic volcanism and modern hydrothermal activity. They also correlate with crustal low-density and low-velocity anomalies. The upper mantle contains an anomalous low-resistivity zone that represents a shallow asthenosphere that contains a small amount of partial melt. The results are consistent with modern geochemical and geophysical data, which show a thin lithosphere below the Hangai region, and geodynamic models that require a low-heat flux asthenospheric upwelling that thermally modifies the lithospheric mantle to explain uplift and volcanism.

## INTRODUCTION

The Hangai Dome in central Mongolia is an intra-continental plateau with a large topographic bulge extending more than 2000 m above the regional elevation (e.g., Cunningham, 2001). The mechanisms of uplift in the continental interior, away from active tectonic margins, is an open and important question. The Hangai region occupies a unique position in central Asia. It is located between the rigid Siberian craton to the north and the Tibetan Plateau to the south, which has a northward compressional regime to accommodate the India-Asia collision (e.g., Calais et al., 2003). The Hangai region is a pre-Cambrian crustal block that is bounded by large, seismically active, strike-slip faults which accommodate this motion (Cunningham, 2001). Both the northern Bulnay fault and the southern Bogd fault have had intra-continental earthquakes larger than magnitude 8 within the last century (e.g., Calais et al., 2003). Surface deformation from crustal thickening due to northward motion caused by the India-Asia collision can not explain Hangai orogenesis because no significant neo-tectonic deformation has been measured within the Hangai region (Liu and Bird, 2008; Calais et al., 2003).

The Hangai region is characterized by dispersed, low-volume, basaltic volcanism, with ages from the Holocene to the Oligocene (Barry et al., 2003). The onset of the uplift of the Hangai Dome is believed to have been coincident with the beginning of volcanism (e.g., Walker et al., 2007), indicating that the processes may be linked. Seismic studies, supported by analysis on xenoliths from surface lavas, estimate a thin lithospheric (60 – 90 km) and a thick crust (45 – 55 km) below the central Hangai region, as compared to the surrounding area where the crust is ~35 km thick and the lithosphere is 150 – 225 km thick (Petit et al., 2008). Geophysical studies have determined that the Hangai Dome is underlain by anomalously low seismic velocities and characterized by a very low negative Bouguer anomaly (e.g., Tiberi et al., 2008; Chen et al., 2015).

Together, these studies give evidence for a major lower crustal and upper mantle anomaly, and make this region a key location for studying intra-continental mountain building processes linked to crust-mantle interactions. Furthermore, the origin of the Hangai Dome is relevant for other cases of continental uplift and sporadic magmatism worldwide, such as the north-eastern USA (e.g., Liu et al., 2015) and central Europe (e.g., Molnar et al., 2015).

A high-heat flux mantle plume was originally favoured to explain the origin of the high topography and associated volcanism of the Hangai Dome (Windley and Allen, 1993). However, some petrological evidence is inconsistent with a deep-rooted, high-heat flux mantle plume as a viable mechanism, including: dispersed volcanism that exhibits no definable spatial boundaries and lacks age progression; small volumes of magmatism that erupted sporadically; and a lack of xenolith evidence for anomalously high lithospheric temperatures (Barry et al., 2003). Hence alternative explanations are sought. Several mechanisms have been proposed to explain uplift, including: a small scale, low heat-flux mantle upwelling of asthenospheric material due to convective removal of lithosphere (e.g., Barry et al., 2003; Chen et al., 2015) or due to lithospheric removal as the result of an instability (Hunt et al., 2012); crustal thickening from the presence of underplated magmatic rocks (e.g., Petit et al., 2002); a thermal shielding effect, where continental lithosphere prevents convective heat transfer to the surface and causes melting (Petit et al., 2002; Barry et al., 2003); uplift due to dynamic topography caused by a long-wavelength upwelling produced by mantle flow patterns (e.g., Becker and Facenna, 2011; Flament et al., 2012); and, a rigid cratonic block that diverts lithospheric mantle flow driven by India, resulting in lithospheric thinning and uplift (Cunningham, 2001).

Past geophysical studies have focused on seismology and gravity, however additional high-resolution geophysical data are needed to image subsurface structure. Magnetotelluric (MT) data map subsurface electrical resistivity using natural electromagnetic signals (e.g., Chave and Jones, 2012). The resistivity of a rock is highly sensitive to the quantity and composition of fluids, and therefore the MT method is useful for investigating subsurface fluid and melt distribution. Therefore MT data have the potential to distinguish between the possible mechanisms responsible for the uplift of the Hangai Dome.

## MT DATA COLLECTION, ANALYSIS, AND MODELING

A total of 125 MT sites were collected in 2016 to investigate the electrical resistivity beneath the Hangai Dome (Figure 1), the first survey of its kind in Mongolia. Broadband and long period instruments (0.002 – 8,000 s) were used to form a large array (~430 x 150 km) with ~50 km site spacing. Dense telluric-only sites (5 – 15 km spacing) were deployed along several profiles, and inter-site transfer functions (e.g., Munoz and Ritter, 2013) were computed. A long, dense profile crossing the Hangai Dome (A – A', see Figure 1) will be the focus of this paper, with future work focusing on a detailed three-dimensional (3-D) analysis of the entire dataset. The profile is ~430 km long with a site spacing of 5 – 10 km and includes a total of 62 sites. The MT data were high quality and had little noise due to the remote measurement location (Figure DR1), however several sites exhibited distortions, indicative of complex local structure (Figure DR2).

The dimensionality of the MT data was investigated using both tensor decomposition and phase tensor methods (e.g., Chave and Jones, 2012; Figure DR3). The short period MT data ( $< 1$  s) sample the upper crustal structure and show no preferred geo-electric strike direction, indicating a fairly homogenous resistivity structure. Longer period data (1 - 1000 s), which sample lower crustal and upper mantle depths, show an average geo-electric strike direction of N105°E. The strike direction is geologically plausible because it is approximately orogeny-parallel, parallel to the main fault zones in the area (Walker et al., 2007), and consistent with seismic anisotropy results (Barruol et al., 2008). Induction vector analysis using vertical magnetic fields supports this strike direction (Figure DR5). The dimensionality analysis established that a two-dimensional (2-D) analysis is valid, although certain regions display local 3-D resistivity structure (Figure DR6), specifically the central region of the profile, below the Hangai Dome, and the southern portion of the profile.

A 2-D electrical resistivity model was created from the MT data (Figure 2) by applying the EMILIA inversion algorithm from Kalscheuer et al. (2010). The algorithm is capable of properly handling inter-site transfer functions computed for the telluric only sites. All depths are below the average surface elevation, defined as 2000 m. A total misfit of 2.51 was achieved, indicating an acceptable fit of the model to the measured MT data (Figure DR10). Model parameters, resolution, and sensitivity was investigated thoroughly and the robustness of the main model features was tested. More details of the inversion can be found in the Supplementary Material.

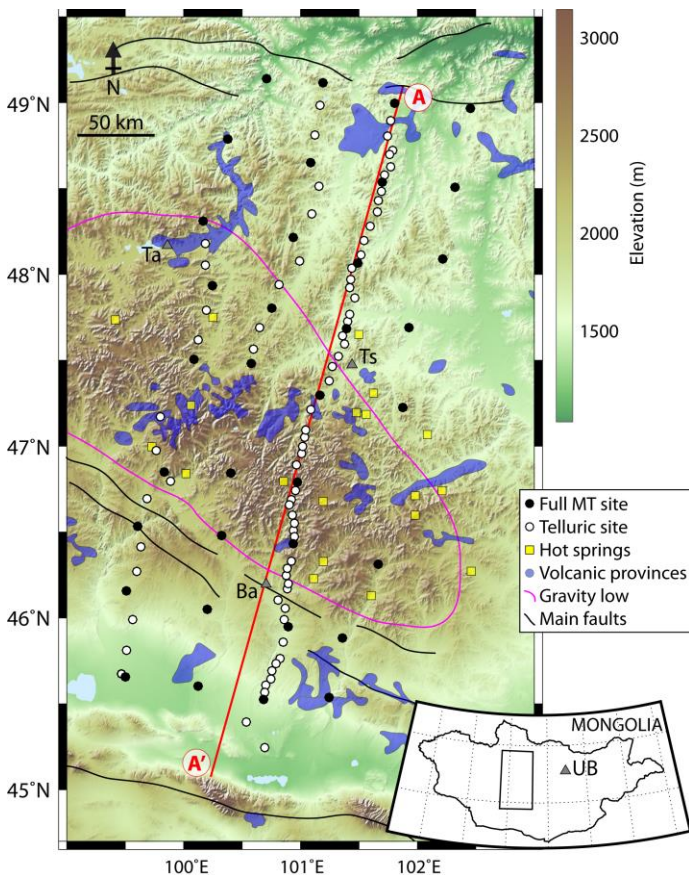


**Figure 1.** Topographic map of the study area; inset map shows location within Mongolia. Magnetotelluric (MT) sites (circles) and profile A-A' (red line) are marked. Ta = Tariat; Ts = Tsetserleg; Ba = Bayankhongor; UB = Ulaanbataar. Additional information includes: volcanic provinces (blue; Sahagian et al., 2014); hot springs (gold; Ganbat and Demberel, 2010); low Bouguer gravity anomaly (pink line; Tiberi et al., 2008); main faults (black lines; Walker et al., 2007; Ganbat and Demberel, 2010).

## RESULTS AND DISCUSSION

The 2-D resistivity model derived from the MT data (Figure 2) reveals several interesting conductive anomalies, described here and discussed in more detail below. Conductive anomalies can have many causes, including aqueous fluids, partial melts, or hydrothermal alteration, and therefore any interpretation must use additional information to distinguish between all possibilities (e.g., Chave and Jones, 2012). The near-surface layer (C1;  $< 0.5$  km) has a highly variable resistivity ( $\sim 100 - 1000 \Omega\text{m}$ ). It is likely caused by a shallow hydrothermal system and sediment infill in wide valley bottoms (e.g., Ganbat and Demberel, 2010). It is underlain by an upper crustal resistor (R1;  $3,000 - 30,000 \Omega\text{m}$ ) that can be explained by highly-resistive pre-Cambrian cratonic basement rocks (Cunningham, 2001). A heterogeneous conductive zone (C2;  $< 100 \Omega\text{m}$ ) that contains pockets of low-resistivity material ( $10 - 30 \Omega\text{m}$ ) is imaged at lower crustal depths of 30 - 50 km. Upper mantle depths are characterized by a moderate resistivity ( $100 - 300 \Omega\text{m}$ ). At depths greater than  $\sim 70$  km a localized conductive feature (C3;  $30 - 100 \Omega\text{m}$ ) is imaged. MT data can give a reliable estimate of the depth to the top of a conductor, but it is not always possible to detect the base of a conductor, because MT signals diffuse in the Earth and their depth of investigation is dependent on both the period of the electromagnetic fields measured and the resistivity of the medium. Therefore, there is no resolution within or below C3, and the overall resolution is reduced below a depth of approximately 150 km.

### Lower crustal conductor

The lower crust beneath the Hangai Dome is a heterogeneous conductive zone and this heterogeneity is well resolved by the dense MT site spacing of 5 - 10 km. It is believed to be a broad zone of fluids and partial melts, and suggests local, discrete accumulations of fluid within the crust. The depth to the top of C2 is coincident with the estimated brittle-ductile transition zone depth of 25 - 35 km (Calais et al., 2003; Petit et al., 2002), and crustal fluids tend to pool near this zone (e.g., Connolly and Podlachikov, 2004). Lava geochemistry from the Hangai region gives evidence for the onset of crystal fractionation at a depth of 25 - 30 km (Hunt et al., 2012), implying that melt storage may have occurred at these depths. However, some geochemical evidence is inconsistent with long-lived crustal melt storage below the Hangai (Harris et al., 2010). Additionally, little to no geochemical fractionation correlation is seen between individual volcanic provinces (Hunt et al., 2012), indicating that magma batches did not interact with each other in the crust. No spatial or temporal changes in the geochemistry of the lavas is observed across the Hangai Dome, and crustal assimilation and contamination appears limited, suggesting that all erupted lavas were sourced directly from a single parent source at mantle depths (Hunt et al., 2012).

A detailed interpretation of the small-scale discrete structures within this zone is difficult. Their geometry and positions, however, are fairly robust, since they are required in all modeling trials, including when a sparser site spacing is used, implying that they are not due to macro-anisotropy effects, or inversion artefacts. Their positions appear to be related to surface expressions of volcanism (Cunningham, 2001; Hunt et al., 2012) and present-day hydrothermal activity (Ganbat and Demberel, 2010), as shown in Figure 2. Melt pathways would have passed through the crust to surface vents, likely along crustal weaknesses, and although magma is likely no longer present, anomalous conductivity due to hydrothermal alteration from past eruptive events can be detected (Comeau et al., 2016; Hill et al., 2009). However, the rapid ascent of magma through the crust in transient pathways (Harris et al., 2010) would not produce a very strong conductive anomaly. Vertically elongated conductive features observed in the upper crust (such as C4, see Figure 2) may represent these past conduits of vertical melt motion.

Joint inversion of gravity and teleseismic data produces models which depict a low-velocity and low-density structure directly below the central Hangai (Tiberi et al., 2008). A careful look at the models shows the lowest velocities are confined to several discrete zones at depths of 0 - 15 km and 30 - 60 km, while the lowest densities occur within depths

of 20 – 80 km (Tiberi et al., 2008). These anomalies are approximately coincident with the conductive zones C2 and C4. The presence of both saline fluids and partial melt will lower the electrical resistivity and also the seismic S-wave velocity and the bulk density (Unsworth and Rondenay, 2012), and so these anomalies are assumed to be due to the same features. These studies, however, used a very broad site spacing (>50 km) and thus lack the fine resolution possible in the resistivity model.

### Upper mantle conductor

The upper mantle features a localized conductive feature (C3) directly below the Hangai Dome, imaged at a depth of more than 70 km with its bottom unconstrained. It is believed to represent a shallow asthenosphere that contains a small amount of partial melt and may represent a zone of melt generation. This is supported by geochemical analysis that indicates the basaltic lavas found across the Hangai Dome have originated by partial melting over prolonged periods from an isolated sub-lithospheric mantle source at depths of 70 – 100 km (Barry et al., 2003; Hunt et al., 2012).

Seismic tomography data detect a thin lithosphere below the Hangai region (60 – 90 km) that thickens rapidly at the edges (up to 150 – 225 km; Tiberi et al., 2008; Petit et al., 2008). Bouguer gravity models reveal a low-density structure at a depth of 80 – 125 km below the central Hangai (see Figure 1; Tiberi et al., 2008). Modern adjoint tomography analysis detected a continuous, broad, low-velocity zone at depths above 150 km, with the lowest shear-wave velocities occurring at depths of 60 – 90 km (Chen et al., 2015). Moreover, this low-velocity zone exhibits strong positive radial anisotropy (5 - 10%), indicating horizontal migration of melt (Chen et al., 2015). These broad surveys image deep structure but lack fine resolution and are prone to smearing over a spatial volume. However C3, although its exact geometry is not well constrained by the resistivity model, is broadly coincident with both of these geophysical anomalies.

### Presence of fluids and partial melt

Low-resistivity anomalies can be explained by the presence of aqueous fluids and/or partial melts. Assuming that the low-resistivity anomalies below the Hangai Dome are due primarily to partial melting, we can infer the melt fraction required to explain the observed bulk electrical resistivity, following the analysis of Comeau et al. (2016). The bulk resistivity measured depends on the amount of melt present, the geometrical melt distribution, and the pure melt resistivity, that in turns depends on the melt's chemical composition, temperature, and pressure (Pommier and Le-Trong, 2011; see Supplementary Material). Geochemical analysis of lava samples from the Hangai Dome, taken to be typical of the anomalous regions at depth, provide constraints on composition and temperature (e.g., Barry et al., 2003; Ionov, 2002), allowing the computation of pure melt resistivity from laboratory databases (Pommier and Le-Trong, 2011; Figure DR11).

Assuming a high degree of interconnection, which is generally true for lithospheric melts (e.g., Unsworth and Rondenay, 2012), and a bulk resistivity of 30  $\Omega\text{m}$ , typical of the conductive anomalies observed, a minimum of 2 - 5% melt is required to explain the electrical resistivity data of the lower crustal conductive zone C2 (see Figure DR12). This is consistent with prior studies that estimated the presence of 2 - 3% melt in the lower crust (Chen et al., 2015). A similar analysis shows that the deeper conductive zone C3 requires a minimum of 4 - 8% melt. This is consistent with prior studies that estimated 3 - 7% melting at depths of 70 – 120 km (Hunt et al., 2012) and possibly up to 12% (Barry et al., 2003). Saline aqueous fluids in addition to partial melt may help explain the observed low-resistivity values. Furthermore, aqueous fluids lower the melting point of the crust and, combined with an increase in heat, could facilitate partial melting (e.g., Unsworth and Rondenay, 2012). The crustal anomaly C2 could be caused entirely by fluids, which were perhaps exsolved from melts or magma at greater depths.

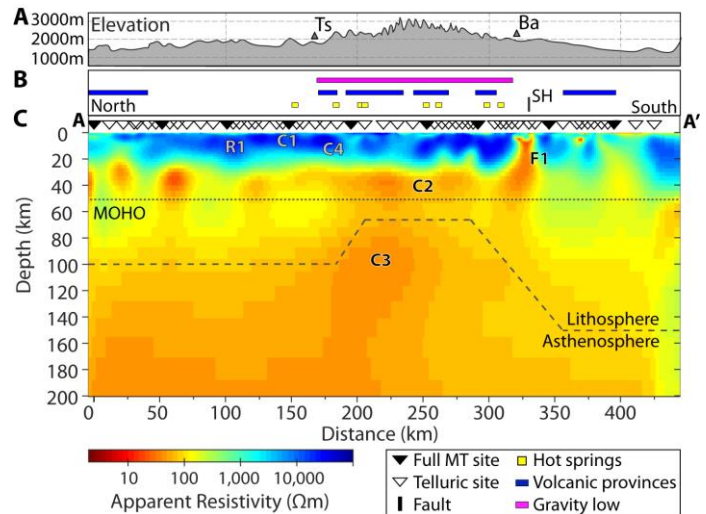


**Figure 2:** **A:** Elevation along profile A-A'. Ts = Tsetserleg; Ba = Bayankhongor. **B:** Additional information projected on the profile: low Bouguer gravity anomaly (pink; Tiberi et al., 2008); volcanic provinces (blue; Sahagian et al., 2014); hot springs (gold; Ganbat and Demberel, 2010); South Hangai fault zone (SH, black line; Walker et al., 2007). **C:** The resistivity model obtained from the inversion of magnetotelluric (MT) data at 62 sites (triangles) along profile A-A'. Dotted line indicates approximate location of crust-mantle boundary (Moho) and dashed line indicates approximate lithosphere-asthenosphere boundary (Petit et al., 2008).

### South Hangai fault zone

Anomalous MT data are seen at several locations on the southern portion of the profile and a conductive feature (~30  $\Omega\text{m}$ ; F1 on Figure 2) stretches vertically through the crust to the surface. This is believed to be the South Hangai fault zone that is observed at the southern edge of the Hangai Dome (e.g., Walker et al., 2007; Cunningham, 2001). Because this fault is a zone of weakened crust it likely has circulating fluids that increase conductivity. The surface expression of this fault is marked on Figure 1, however internal deformation is distributed over a wider area. The abrupt edge of the lower crustal conductive zone C2 occurs at the same location, implying that it is confined below the Hangai Dome and signifying the importance of this fault zone. The large faults that bound the Hangai region are believed to be lithospheric-scale (Calais et al., 2003), and so the contrasting crustal properties observed on either side of this fault likely reflect the rheological differences between the strong Hangai block and the weaker terranes to the south (Cunningham, 2001). The depth to the conductive zone C3 increases rapidly at this location, indicating a thicker lithosphere south of the Hangai region, consistent with seismic results (e.g., Petit et al., 2008).

### IMPLICATIONS AND CONCLUSIONS

The MT-derived resistivity model (Figure 2) gives new constraints on the structure beneath the Hangai Dome and can be used to distinguish between proposed uplift mechanisms. It is possible that a high-heat flux mantle plume was active in the past, for example during early magmatism as proposed by Barry et al. (2003), but has waned, because no such feature is observed today. The moderate resistivity values observed in this study imply low percent partial melting and suggest a low temperature anomaly. A thick layer (<20 km) of underplated basalt could explain uplift and magmatism (Chen et al., 2015; McKenzie, 1984). However, it is unlikely because the required electrical signature of a homogenous sub-crustal high-conductivity zone (Wannamaker et al., 2008) is not observed. Furthermore, the relatively low temperatures estimated at the base of the crust are inconsistent with underplated basaltic melts (Ionov, 2002). The resistivity model also presents no direct evidence for a thick, rigid crustal keel, as suggested by Cunningham (2001), and this hypothesis cannot explain the observed deep conductive anomaly. A cratonic thermal



shielding effect (Petit et al., 2002) is not consistent with the geometry or location of the deep conductive anomaly detected. Uplift and doming due to dynamic topography (e.g., Flament et al., 2012) is consistent with the mantle flow models of Becker and Facenna (2011) and is not ruled out by the MT data. However, the mantle upwelling depicted in the resistivity model has a much smaller wavelength than that predicted by dynamic topography models. Hot and buoyant asthenospheric material replacing delaminated or removed lithospheric material could explain uplift and doming of the Hangai region (Barry et al., 2003; Hunt et al., 2012). A small-scale (~100 km wide) asthenospheric upwelling is consistent with the resistivity model.

Therefore, our preferred model favors a low-heat flux, small-scale asthenospheric upwelling as the mechanism for uplift. Low-percent partial melts (i.e., 4 - 12%) are generated due to decompression melting at a location near C3 and melt migrating laterally within the upper mantle (Chen et al., 2015) and excess heat cause thermal modification over a large region below the Hangai Dome. Both seismic and gravity data support this model (e.g., Chen et al., 2015; Tiberi et al., 2008) and geochemical constraints from mantle xenoliths erupted in past volcanic events are in agreement (e.g., Ionov, 2002). However what initiated the process remains speculative.

The MT-derived 2-D resistivity model presented here is consistent with previous geochemical and geophysical studies over the Hangai Dome, but adds new, complementary information. Future work will further refine this model with the continued analysis of the full 3-D dataset over the entire Hangai Dome. Furthermore, MT data can provide constraints on lithospheric viscosity and mechanical strength, both of which are required for accurate modeling of lithosphere dynamics (e.g., Liu and Hasterok, 2016), and future work will move in this direction.

## ACKNOWLEDGEMENTS

This research was financially supported by DFG grant #BE 5149/6-1 and SNF grant #200021L\_162660/1. We thank Thomas Kalscheuer for the 2-D MT inversion code. We thank the Geophysical Instrument Pool Potsdam for the use of their MT instruments. We thank those who helped collect the data and provided field support, including Batbileg, Nomuun, Dominic, Dorian, Neeraj, Joerg, Eldev-Ochir, Gantsogt, Tsagaansukh, Zagdsuren, and other members of the Mongolian Academy of Science.

## REFERENCES CITED

Barry, T.L., Saunders, A.D., Kempton, P.D., Windley, B.F., et al., 2003, Petrogenesis of Cenozoic Basalts from Mongolia: Evidence for the Role of Asthenospheric versus Metasomatized Lithospheric Mantle Sources: *J. Petrol.*, v. 44, p. 55-91.

Barruol G., Deschamps, A., Deverchère, J., Mordinova, V., et al., 2008, Upper mantle flow beneath and around the Hangay dome, Central Mongolia: *Earth Planet. Sci. Lett.*, v. 274, p. 221-233.

Becker, T.W., and Facenna, C., 2011, Mantle conveyor beneath the Tethyan collisional belt: *Earth Planet. Sci. Lett.*, v. 310, p. 453-461.

Calais E., Vernolle, M., San'kov, V., Lukhnev, A., et al., 2003, GPS measurements of crustal deformation in the Baikal-Mongolia area (1994–2002): Implications for current kinematics of Asia: *J. Geophys. Res.*, v. 108, p. 1-14.

Chave, A.D., and Jones, A.G., eds., 2012, *The magnetotelluric method: Theory and practice*: Cambridge, Cambridge University Press, 552 p.

Chen, M., F. Niu, Q. Liu, J. Tromp, 2015, Mantle-driven uplift of Hangai Dome: New seismic constraints from adjoint tomography: *Geophys. Res. Lett.*, v. 42.

Comeau, M. J., Unsworth, M. J., Cordell, D., 2016, New constraints on the magma distribution and composition beneath Volcán Uturuncu and the southern Bolivian Altiplano from magnetotelluric data: *Geosphere*, v. 12(5), p. 1391-1421.

Connolly, J.A.D., and Podlachikov, Y.Y., 2004, Fluid flow in compressive tectonic settings: Implications for midcrustal seismic reflectors and downward fluid migration: *J. Geophys. Res.*, v. 109(B4).

Cunningham, W.D., 2001, Cenozoic normal faulting and regional doming in the southern Hangay region, Central Mongolia: implications for the origin of the Baikal rift province: *Tectonophysics*, v. 331, p. 389-411.

Flament, N., Gurnis, M., Muller, R. D., 2012, A review of observations and models of dynamic Topography: *Lithosphere*, v. 5(2), p. 189-210.

Ganbat E., and Demberel, O., 2010, Geologic Background of the Hangay Geothermal System, West-Central Mongolia: *Proceedings World Geothermal Congress 2010, Bali, Indonesia, 25-29 April 2010*.

Harris, N., Hunt, A., Parkinson, I., Tindle, A., Yondon, M., Hammond, S., 2010, Tectonic implications of garnet-bearing mantle xenoliths exhumed by Quaternary magmatism in the Hangay dome, central Mongolia: *Contrib. Mineral. Petr.*, v. 160, p. 67-81.

Hill, G.J., Caldwell, T.G., Heise, W., Chertkoff, D.G., et al., 2009, Distribution of melt beneath Mount St Helens and Mount Adams inferred from magnetotelluric data: *Nature Geoscience*, v. 2, p. 785-789.

Hunt, A.C., Parkinson, I.J., Harris, N., Barry, T.L., Rogers, N.W., Yondon, M., 2012, Cenozoic Volcanism on the Hangai Dome, Central Mongolia: Geochemical Evidence for Changing Melt Sources and Implications for Mechanisms of Melting: *J. Petrol.*, v. 53(9), p. 1913-1942.

Ionov, D., 2002, Mantle structure and rifting processes in the Baikal–Mongolia region: geophysical data and evidence from xenoliths in volcanic rocks: *Tectonophysics*, v. 351, p. 41–60.

Kalscheuer, T., Juanatey, M.D.A.G., Meqbel, N., Pedersen, L.B., 2010, Non-linear model error and resolution properties from two-dimensional single and joint inversions of direct current resistivity and radiomagnetotelluric data: *Geophys. J. Int.*, v. 182 (3), p. 1174-1188.

Liu, Z., Bird, P., 2008, Kinematic modelling of neotectonics in the Persia–Tibet–Burma Orogeny: *Geophys. J. Int.*, v. 172, p. 779-797.

Liu S., King, S., Adam, C., Long, M., Benoit, M., Kirby, E., 2015, Mantle Flow Pattern and Dynamic Topography beneath the Eastern US: Abstract #T11D-2934 presented at 2015 Fall Meeting, AGU, San Francisco, USA.

Liu, L., Hasterok, D., 2016, High-resolution lithosphere viscosity and dynamics revealed by magnetotelluric imaging: *Science*, v. 353, p. 1515-1518.

McKenzie, D., 1984, A possible mechanism for epeirogenic uplift: *Nature*, v. 307, p. 16.

Molnar, P., England, P.C., Jones, C.H., 2015, Mantle dynamics, isostasy, and the support of high terrain: *J. Geophys. Res.*, v. 120, p. 1932–1957.

Munoz, G., Ritter, O., 2013, Pseudo-remote reference processing of magnetotelluric data: a fast and efficient data acquisition scheme for local arrays: *Geophys. Prospect.*, v. 61, p. 300-316.

Petit, C., Tiberi, C., Deschamps, A., Deverchère, J., 2008, Teleseismic traveltimes, topography and the lithospheric structure across central Mongolia: *Geophys. Res. Lett.*, v. 35, p. 1-5.

Petit, C., Déverchère, J., Calais, E., Sankov, V., Fairhead, D., 2002, Deep structure and mechanical behavior of the lithosphere in the Hangai–Hövsögöl region, Mongolia: new constraints from gravity modeling: *Earth Planet. Sci. Lett.*, v. 197, p. 133–149.

Pommier, A., and Le-Trong, E., 2011, SIGMELTS: A web portal for electrical conductivity calculations in geosciences, *Comput. Geosci.*, v. 37, p. 1450–1459.

Sahagian, D., Proussevitch, A., Ancuta, L., Idleman, B., Zeitler, P., 2014, Mongolian Hangay Uplift Recorded in Vesicular Basalts: Abstract #T21A-4558 presented at 2014 Fall Meeting, AGU, San Francisco, USA.

Tiberi, C., Deschamps, A., Déverchère, J., Petit, C., Perrot, J., Appriou, D., 2008, Asthenospheric imprints on the lithosphere in Central Mongolia and Southern Siberia from a joint inversion of gravity and seismology (MOBAL experiment): *Geophys. J. Int.*, v. 175, p. 1283-1297.

Unsworth, M.J., and Rondenay, S., 2012, Mapping the distribution of fluids in the crust and lithospheric mantle utilizing geophysical methods, in Harlov, D.E., and Austrheim, H., eds., *Metasomatism and the Chemical Transformation of Rock*, Lecture Notes in Earth System Sciences, Springer Verlag, Berlin, p. 535-598.

Walker, R.T., Nissen, E., Molor, E., Bayasgalan, A., 2007, Reinterpretation of the active faulting in central Mongolia: *Geology*, v. 35, p. 759-762.

Wannamaker, P.E., Hasterok, D.P., Johnston, J.M., Stodt, J.A., et al., 2008, Lithospheric dismemberment and magmatic processes of the Great Basin–Colorado Plateau transition, Utah, implied from magnetotellurics: *Geochem. Geophys. Geosyst.*, v. 9.

Windley, B.F., and Allen, M.B., 1993, Mongolian plateau: Evidence for a late Cenozoic mantle plume under central Asia, *Geology*, v. 21, p. 295-298.

<sup>1</sup>GSA Data Repository item 2017xxx, Supporting documentation, related figures, and an explanations of methods is available online at [www.geosociety.org/pubs/xxxx.htm](http://www.geosociety.org/pubs/xxxx.htm), or on request from [editing@geosociety.org](mailto:editing@geosociety.org) or Documents Secretary, GSA, P.O. Box 9140, Boulder, CO 80301, USA.